Analytical technique for determining the polarization dependence of optical matrix elements in quantum wires with band-coupling effects

Peter C. Sercel and Kerry J. Vahala
Department of Applied Physics, Mail Stop 128-95, California Institute of Technology, Pasadena, California 91125

(Received 13 March 1990; accepted for publication 29 May 1990)

We present an analytical technique for determining polarization-dependent optical transition matrix elements in quantum wires which rigorously incorporates the effects of band coupling. Using this technique, we examine the polarization anisotropy of the two lowest energy optical transitions in a GaAs quantum wire. Contrary to assumptions employed in previous studies, we show that the valence states involved in these transitions are a strong admixture of light and heavy hole character. The lowest energy transition is found to be four times stronger for electric fields oriented parallel to the wire than for the perpendicular orientation. In contrast, the next highest transition does not interact with optical waves polarized along the wire axis. We discuss sources of error which arise in simpler one-band models of this phenomenon in addition to the neglect of band coupling and show that the coupled band model presented here is essential for predicting these effects.

Polarization-dependent photoluminescence excitation (PLE) spectroscopy has emerged recently as a powerful tool for the characterization of quantum wires.[1,2] In particular, these PLE studies have shown that a strong anisotropy exists in the relative intensity of the two lowest energy exciton lines in quantum wire arrays as a function of polarization of the exciting light. Given the importance of this observation to future application of quantum wires (or quantum dots) to semiconductor lasers,[3–7] it is crucial that a rigorous theoretical understanding of this effect be established. However, the theoretical model which has previously been used to interpret this effect contains two major simplifications whose validity has so far not been examined: band coupling effects are neglected in order to render the calculation tractable, and coherence terms are neglected in the calculation of the optical transition matrix element.

In this letter we apply a new analytical coupled-band formalism[8,9] to determine polarization dependence of optical matrix elements in cylindrical quantum wires. We find that the polarization anisotropy reported in Refs. 1 and 2 is well explained by the coupled band model presented here. However, our result shows that the neglect of band coupling effects in previous analyses[1,2,4,5] is incorrect, despite reported agreement of the one-band theory with experiment. A critical examination of the one-band model used in Refs. 1, 2, 4, and 5 finds an unjustified neglect of coherence terms in the transition matrix element. When these coherence terms are retained, the one-band model does not explain the observed anisotropy. A correct understanding of polarization anisotropy in quantum wires requires a coupled band approach such as that presented here.

Our approach is to derive analytic expressions for quantum wire eigenstates at the conduction and valence subband edges and to determine the optical transition matrix element between these states. Beginning with the valence bands, we follow the treatment of Refs. 8 and 9 and write a Luttinger-type Hamiltonian for the coupled Γ_8 states in a representation not of Bloch plane waves, but of the appropriate cylindrical waves. These are eigenstates of the operator $\mathbf{F}_z$, the projection of total angular momentum along the z axis. The total angular momentum operator is defined by the relation $\mathbf{F} = \mathbf{J} + \mathbf{L}$, where $\mathbf{J}$ is the angular momentum of zone-center Bloch functions $|J, J_z\rangle$, with quantum number $J = 3/2$ for the Γ_8 states,[10] and $\mathbf{L}$ is the angular momentum of the envelope part of the total wave function.[9,11] In a spherical band structure approximation,[12] F_z is a good quantum number so the Hamiltonian in this basis is block diagonal. Using the fact that $\mathbf{F}_z = \mathbf{J}_z + \mathbf{L}_z$ we construct the necessary basis in the product form

$$|K_z,k,F_z;J,J_z\rangle = |J,J_z\rangle|K_z;k,L_z = F_z - J_z\rangle\,, \tag{1}$$

where the envelope vector $|K_z; k, L_z\rangle$ is represented in cylindrical coordinates by

$$\langle r,\theta,z|K_z;k,L_z\rangle = (i^{L_z}/2\pi)J_{L_z}(kr)e^{iL_z\theta}e^{iK_z z}\,. \tag{2}$$

Here k is radial wave number, J_{L_z} is a Bessel function of order L_z, and K_z is the down-wire crystal momentum of the envelope.

We specialize now in the case of zero down-wire momentum ($K_z = 0$), since the optical properties of the quantum wire are predominantly determined by the states at the subband edges. In the new basis Eq. (1), each subblock $\mathbf{H}^{\Gamma_8}_{F_z}(K_z = 0)$ of the Γ_8 Hamiltonian assumes the identical form:[9]

$$\mathbf{H}^{\Gamma_8}_{F_z}(K_z=0) = \begin{array}{c} \\ \\ \\ \\ \end{array} \begin{array}{c} |3/2,3/2\rangle|F_z-3/2\rangle \\ |3/2,-1/2\rangle|F_z+1/2\rangle \\ |3/2,-3/2\rangle|F_z+3/2\rangle \\ |3/2,1/2\rangle|F_z-1/2\rangle \end{array} \begin{pmatrix} E_v-(\gamma_1+\gamma_2)(k^2/2) & \sqrt{3}\gamma_2(k^2/2) & 0 & 0 \\ \sqrt{3}\gamma_2(k^2/2) & E_v-(\gamma_1-\gamma_2)(k^2/2) & 0 & 0 \\ 0 & 0 & E_v-(\gamma_1-\gamma_2)(k^2/2) & \sqrt{3}\gamma_2(k^2/2) \\ 0 & 0 & \sqrt{3}\gamma_2(k^2/2) & E_v-(\gamma_1+\gamma_2)(k^2/2) \end{pmatrix}, \tag{3}$$

 0003-6951/90/320545-03$02.00

where we omit indices K_z, k in the basis vectors. The γ's in the matrix are the familiar Luttinger parameters written in the spherical band structure approximation ($\gamma_2 = \gamma_3$).[12] The matrix is decoupled into two 2×2 subblocks of opposite envelope parity. The eigenvectors are, for the heavy holes,

$$|\mathrm{HH1}\rangle_{F_z} = \tfrac{1}{2}\{|3/2,3/2\rangle|F_z - 3/2\rangle + \sqrt{3}|3/2,-1/2\rangle|F_z + 1/2\rangle\}$$
$$|\mathrm{HH2}\rangle_{F_z} = \tfrac{1}{2}\{|3/2,-3/2\rangle|F_z - 3/2\rangle + \sqrt{3}|3/2,1/2\rangle|F_z - 1/2\rangle\} \quad (4)$$

with eigenvalue $E_{\mathrm{HH}} = E_v - (\gamma_1 - 2\gamma_2)k^2/2$. The numbers 1(2) in the vectors refer to the upper left (lower right) subblocks of Eq. (3). For the light holes, the eigenvectors are

$$|\mathrm{LH1}\rangle_{F_z} = \tfrac{1}{2}\{-\sqrt{3}|3/2,3/2\rangle|F_z - 3/2\rangle + |3/2,-1/2\rangle|F_z + 1/2\rangle\}$$
$$|\mathrm{LH2}\rangle_{F_z} = \tfrac{1}{2}\{-\sqrt{3}|3/2,-3/2\rangle|F_z + 3/2\rangle + |3/2,1/2\rangle|F_z - 1/2\rangle\} \quad (5)$$

with eigenvalue $E_{\mathrm{LH}} = E_v - (\gamma_1 + 2\gamma_2)(k^2/2)$.

To form quantum wire eigenstates, we superpose light and heavy hole vectors inside and outside the wire. The zone-center quantum wire eigenstates are generally superpositions of bulk heavy and light hole vectors of given parity:

$$\psi^1_{V(F_z)} = A_1|\mathrm{HH1}\rangle_{F_z} + B_1|\mathrm{LH1}\rangle_{F_z}$$
$$\psi^2_{V(F_z)} = A_2|\mathrm{HH2}\rangle_{F_z} + B_2|\mathrm{LH2}\rangle_{F_z}. \quad (6)$$

Utilizing the envelope representation given in Eq. (2), the requirement of continuity of total wave function and probability current at the surface of the wire, $r = R$, leads to a dispersion relation which determines the subband edge energy for a particular state.[9] For simplicity, in what follows we assume infinite well depth. In this case, the dispersion relation for even parity states of quantum number $F_z = 1/2$ is:

$$3J_0[k_{\mathrm{HH}}(E)R\,]J_2[k_{\mathrm{LH}}(E)R\,] + J_0[k_{\mathrm{LH}}(E)R\,]J_2[k_{\mathrm{HH}}(E)R\,] = 0, \quad (7)$$

while for $F_z = 3/2$, the even parity states obey

$$3J_2[k_{\mathrm{HH}}(E)R\,]J_0[k_{\mathrm{LH}}(E)R\,] + J_2[k_{\mathrm{LH}}(E)R\,]J_0[k_{\mathrm{HH}}(E)R\,] = 0, \quad (8)$$

Solution of these equations for a given wire radius yields the result that the highest energy state (i.e., lowest hole confinement energy) corresponds to $F_z = 1/2$, even parity, while the next highest state is the $F_z = 3/2$, even parity state.[9] Using the energies determined with Eqs. (7) and (8) it is then straightforward to compute the heavy and light hole amplitudes in Eqs. (6) which normalize the wave functions. In the infinite barrier approximation, the highest state, corresponding to $F_z = 1/2$, has only 41% heavy hole character, versus 67% heavy hole character for the next highest state, with quantum number $F_z = 3/2$. Use of a finite barrier will change these numbers in a minor way; for a 10-nm-diam GaAs wire embedded in $Al_{0.3}Ga_{0.7}As$ the numbers quoted above are changed to 30 and 68% heavy hole character, respectively. Thus the neglect of band mixing in previous quantum wire calculations can be expected to cause serious errors.

We now calculate the optical transition matrix element between the even parity valence states just discussed and the lowest conduction-band state at zone center, which has even parity and twofold degeneracy ($F_z = \pm 1/2$). Since parity provides a selection rule at zone center, transitions involving the odd parity valence states are forbidden; hence we omit discussion of such transitions. Assuming infinite well depth, the two degenerate conduction wave functions are given by

$$\psi_{C(\pm\frac{1}{2})} = (1/N_C)J_0[\alpha_{0,1}(r/R)\,]|1/2,\pm 1/2\rangle, \quad (9)$$

where $\alpha_{0,1}$ is the first root of the zeroth-order Bessel function and N_C normalizes the wave function. The effective squared transition matrix element thus takes the general form

$$|M|^2_{C-V(F_z)} = \{|\langle\psi_{C(\frac{1}{2})}|\mathbf{P}|\psi_{V(F_z)}\rangle\cdot\hat{A}\,|^2 + |\langle\psi_{C(-\frac{1}{2})}|\mathbf{P}|\psi_{V(F_z)}\rangle\cdot\hat{A}\,|^2\}. \quad (10)$$

Here $\hat{A}$ is the polarization vector of the linearly polarized optical wave, which we take to be $\mathbf{A} = \cos(\theta)\hat{z} + \sin(\theta)\hat{x}$, where z is the wire axis, and $\psi_{V(F_z)}$ is one of the valence wave functions of the form given in Eq. (6).

We can now write the polarization-dependent effective optical matrix element for transitions between $\psi_{C(\pm\frac{1}{2})}$ and the $F_z = 1/2$ and $F_z = 3/2$ valence states of Fig. 1. Using the explicit representations $|1/2,1/2\rangle = |s\rangle\uparrow, |1/2,-1/2\rangle = |s\rangle\downarrow, |3/2,3/2\rangle = -\sqrt{1/2}(|x\rangle + i|y\rangle)\uparrow$, and $|3/2,-1/2\rangle = \sqrt{1/6}(|x\rangle - i|y\rangle)\uparrow + \sqrt{2/3}|z\rangle\downarrow$, we find

$$|M|^2_{C-V(\frac{3}{2})} = \tfrac{1}{2}\sin^2(\theta)|P|^2 I^2_{C-V(\frac{3}{2})}, \quad (11)$$

$$|M|^2_{C-V(\frac{1}{2})} = (\tfrac{2}{3}\cos^2(\theta)|P|^2 + \tfrac{1}{6}\sin^2(\theta)|P|^2)I^2_{C-V(\frac{1}{2})}, \quad (12)$$

where, in the subscripts, the valence state is labeled $V(F_z)$. P is the momentum matrix element between orbital 's' and 'p' states[10] and the "I" are the overlap integrals. For GaAs with infinite well depth we find $I_{C\text{-}V(\frac{3}{2})} = 0.991$ and $I_{C\text{-}V(\frac{1}{2})} = 0.821$, independent of wire radius. For a finite well depth these expressions are unchanged exept that the value of the overlap integrals become dependent on the wire radius. For reference, a GaAs wire embedded in $Al_{0.3}Ga_{0.7}As$ with a 10 nm diameter leads to values $I_{C\text{-}V(\frac{3}{2})} = 0.966$ and $I_{C\text{-}V(\frac{1}{2})} = 0.938$.

The relative strengths of these squared optical transition matrix elements are plotted in Fig. 1 as a function of the polarization angle θ measured with respect to the wire axis. Note that the lowest energy transition C-$V(\frac{3}{2})$ is four times stronger for an electric field oriented along the wire than for the perpendicular orientation. The trend is reversed for the transition involving the $F_z = 3/2$ state, which does not interact with electric fields polarized along the wire axis. To connect this result to the PLE studies reported in Refs. 1 and 2, we note that the energy difference between the $F_z = 3/2$ and $F_z = 1/2$ valence states for a given wire radius is consistent with the observed spectral shift between electron-light hole (e-lh) and electron-heavy hole (e-hh) exciton peak assignments made in Refs. 1 and 2 for wires of similar size. The peaks labeled e-lh and e-hh in those studies correspond here to $[C\text{-}V(\frac{3}{2})]$ and $[C\text{-}V(\frac{1}{2})]$, respectively. These new assign-

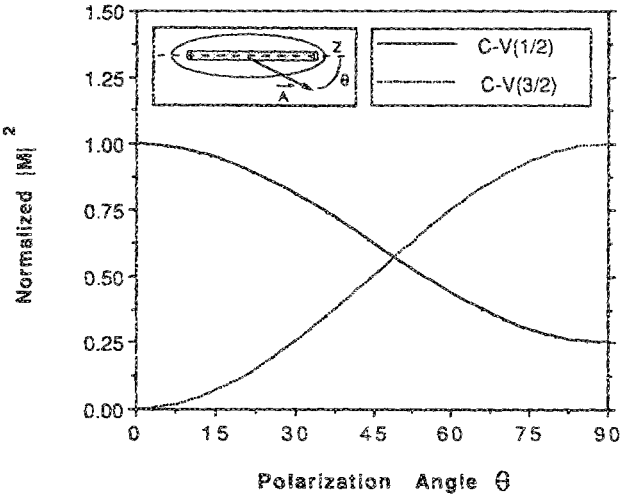

FIG. 1. Normalized squared optical matrix element plotted vs the polarization angle θ measured from the wire axis (i.e., at $\theta = 0$, E is parallel to the wire axis). The curves are for transitions between the lowest electron state and the highest two valence states, $F_z = 1/2$ and $F_z = 3/2$ at $K_z = 0$.

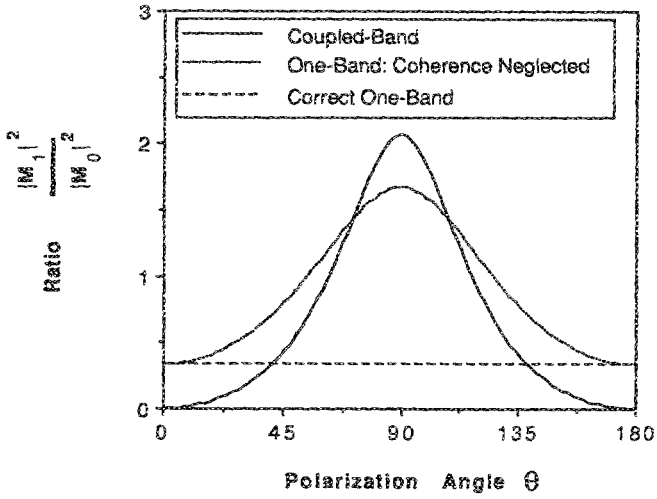

FIG. 2. Relative anisotropy of transition strength for the two lowest energy transitions in a quantum wire. Polarization angle is defined as in Fig. 1. The curve labeled "Coupled-Band" is the ratio of the transition strength of $[C\text{-}V(\frac{3}{2})]$ and $[C\text{-}V(\frac{1}{2})]$. The curve labeled "One-band: Coherence Neglected" shows relative anisotropy of e-lh to e-hh transitions in the one-band model neglecting coherence terms in the matrix element, Eq. (14). "Correct One-Band" refers to Eq. (15) which retains coherence terms in the one-band calculation. For this case there is no relative anisotropy.

ments are accurate within the uncertainty of the wire size and confinement potential in Refs. 1 and 2. Furthermore, a plot of the ratio of Eq. (11) to Eq. (12) as a function of the polarization angle θ, shown in Fig. 2, corresponds closely to the measured data in Refs. 1 and 2.

For comparison, in Fig. 2 we also plot the ratio of the squared [e-lh] and [e-hh] matrix elements calculated in the one-band model of Refs. 1, 2, and 4. In these works, the squared transition matrix element was computed in an infinite well quantum wire structure of square or rectangular cross section for each of the four directions $\mathbf{k}_i$ pointing towards a corner, and then averaged:

$$|M|^2 = \sum_i |\langle 1/2,1/2|\mathbf{P}|U_v(\mathbf{k}_i)\rangle \cdot \hat{A}|^2 . \tag{13}$$

Here, $|U_v(\mathbf{k}_i)\rangle$ is the Bloch function for a heavy or light hole wave corresponding to wavevector $\mathbf{k}_i$.[10] This approach leads to the following expression for the relative squared matrix elements of the e-lh and e-hh transitions:

$$\frac{|M|^2_{e\text{-lh}}}{|M|^2_{e\text{-hh}}} = \frac{\frac{1}{2}\cos^2(\theta) + \frac{5}{4}\sin^2(\theta)}{\frac{3}{2}\cos^2(\theta) + \frac{3}{4}\sin^2(\theta)}, \tag{14}$$

which is equivalent to Eq. (1) of Ref. 1. However, since the waves involved in the summation in Eq. (13) are part of a coherent superposition forming a stationary state in a quantum wire, it is actually not correct to treat them as independent. Equations (13) and (14) neglect this coherence, and should therefore be corrected. This is accomplished by performing the summation in Eq. (13) *before* squaring. For the light and heavy waves, this results in the corrected formula:

$$\frac{|M|^2_{e\text{-lh}}}{|M|^2_{e\text{-hh}}} = \frac{\frac{2}{3}\cos^2(\theta) + \frac{1}{6}\sin^2(\theta)}{2\cos^2(\theta) + \frac{1}{2}\sin^2(\theta)} = \frac{1}{4}, \tag{15}$$

which is *constant* with respect to polarization. The one-band model is therefore incapable of explaining the polarization-dependent absorption observed in Refs. 1 and 2.

In conclusion, we have demonstrated a rigorous coupled-band technique for calculating polarization dependence of optical transition matrix elements in quantum wires. The technique explains observed polarization-dependent PLE data reported in Refs. 1 and 2. We find additionally that the reported agreement between a simple one-band model and the observed data in these studies is a result of incorrectly neglecting coherence terms in the matrix element calculation. When these are included, the one-band model fails to predict a polarization anisotropy between e-lh and e-hh transitions. This fact, coupled with the high degree of admixture of light and heavy hold character into the zone-center valence-subband wave functions reported here, shows clearly that a coupled band model is critical to the understanding of polarization anisotropy in quantum wires.

This work was supported by grants from the Office of Naval Research and the National Science Foundation. P. C. S. would like to acknowledge a NSF graduate fellowship.

[1]M. Tsuchiya, J. M. Gaines, R. H. Yan, R. J. Simes, P. O. Holtz, L. A. Coldren, and P. M. Petroff, Phys. Rev. Lett. **62**, 466 (1989).
[2]Masaaki Tanaka and Hiroyuki Sakaki, Appl. Phys. lett. **54**, 1326 (1989).
[3]Yasuhiko Arakawa, Kerry Vahala, and Amnon Yariv, Appl. Phys. Lett. **45**, 950 (1984).
[4]Masahiro Asada, Yasuyuki Miyamoto, and Yasuharu Suematsu, Jpn. J. Appl. Phys. **24**, L95 (1985).
[5]Masahiro Asada, Yasuyuki Miyamoto, and Yasuharu Suematsu, IEEE J. Quantum Electron. **9**, 1915 (1986).
[6]Kerry J. Vahala, IEEE J. Quantum Electron. **24**, 523 (1988).
[7]Hal Zarem, Kerry J. Vahala, and Amnon Yariv, IEEE J. Quantum Electron. **25**, 705 (1989).
[8]Peter C. Sercel and Kerry J. Vahala, International Quantum Electronics Conference, Anaheim, California 1990, paper QThA2.
[9]Peter C. Sercel and Kerry J. Vahala, to appear in Phys. Rev. B 15.
[10]Evan O. Kane, J. Phys. Chem. Solids **1**, 249 (1957).
[11]A. Baldereschi and Nunzio O. Lipari, Phys. Rev. B **8**, 2697 (1973).
[12]J. M. Luttinger, Phys. Rev. **102**, 1030 (1956).